

# THE PHYSICAL AND TECHNICAL LIMITS OF THE CAPABILITIES OF LOW-TEMPERATURE NON-EQUILIBRIUM PLASMA (LTNP) TECHNOLOGIES OF ATMOSPHERIC PRESSURE

Gosteev S.G.

*Gosteev Sergei Grigorevich – Head of the Department,  
BRANCH  
UNITED ENGINE CORPORATION JSC  
ENGINEERING DESIGN BUREAU "HORIZONT", DZERZHINSKY, MOSCOW REGION*

**Abstract:** *this document examines the presence of natural physical and technical limitations of the technology of low-temperature non-equilibrium plasma of atmospheric pressure created by pulsed-periodic nanosecond corona discharge*

**Keywords:** *low-temperature non-equilibrium plasma, high power pulse-periodic nanosecond corona discharge, energy density of a streamer discharge.*

## ФИЗИКО-ТЕХНИЧЕСКИЕ ПРЕДЕЛЫ ВОЗМОЖНОСТЕЙ ТЕХНОЛОГИЙ НИЗКОТЕМПЕРАТУРНОЙ НЕРАВНОВЕСНОЙ ПЛАЗМЫ (НТПН) АТМОСФЕРНОГО ДАВЛЕНИЯ

Гостеев С.Г.

*Гостеев Сергей Григорьевич – начальник отдела,  
филиал  
АО «Объединённая двигателестроительная корпорация»  
Машиностроительное Конструкторское Бюро «Горизонт», г. Дзержинский, Московская обл.*

**Аннотация:** *в этой статье рассматривается наличие естественных физико-технических ограничений технологии низкотемпературной неравновесной плазмы атмосферного давления, создаваемой импульсно-периодическим наносекундным коронным разрядом.*

**Ключевые слова:** *низкотемпературная неравновесная плазма, мощный импульсно-периодический наносекундный коронный разряд, плотность энергии стримерного разряда.*

*UDC 537.12; 537.523.3; 537.53; 537.563.2*

### 1. Introduction

Currently, a number of gas-discharge techniques are known used in the development of technologies for processing gases, liquids, various surfaces and microbiological objects with chemically active particles of low-temperature non-equilibrium plasma (LTNP): dielectric barrier discharge (DBD), pulse-periodic corona (PPC), high power pulse-periodic nanosecond corona discharge (HPPNCD), HF and microwave discharges and a number of others [1]. The usual form of DBD excited by alternating current is a set of micro-discharges distributed over the surface of the dielectric, each with a duration of 10-15 ns, a diameter of 100-300 microns, a current density of about 100 A/cm<sup>2</sup> in gaps of 1-3 mm. In recent years, it has been possible to obtain a homogeneous discharge DBD in a limited range of parameters. The PPC (often in combination with a dielectric barrier) differs in that at least one of the electrodes has the shape of a tip and is implemented as a streamer that propagates during the pulse up to the opposite electrode. Thus, DBD (in the usual form) and the streamer corona in separate pulses create inhomogeneous gas excitation. Averaging over a set of pulses leads to homogeneous excitation on average. Microwave plasma of critical and subcritical levels with a discharge initiator is also of practical interest.

In most of the electro physical methods being developed recently, discharges formed by PPC are used to create low-temperature atmospheric plasma for surface treatment. However, even in this case, the authors have big problems with the creation and operation of high-voltage electrical equipment necessary to maintain the stability of the discharge, which greatly hinders the introduction of plasma technologies into the industry. Despite the significant progress made in laboratory and pilot scale tests, atmospheric pressure cold plasma treatment has not yet received sufficient development for cost-effective industrial distribution (with the exception of DBD discharge plasma during surface treatment, so in the printing industry there are DBD processing devices with a useful power of up to 30 kW in the equipment market). An obstacle to application is, firstly, that cold plasma sources are technically complex equipment that is not mass-produced. Secondly, the existing methods of plasma treatment can lead to the destruction of materials at the points of contact between the plasma and the treated surface in the case of current lacing.

### 2. High power pulse-periodic nanosecond corona discharge

HPPNCD plasma is devoid of the majority disadvantages. It is characterized by ionization non-equilibrium and nonisothermicity, which are its main energy advantages over other types of discharges. Special measures to prevent lacing of non-equilibrium plasma in HPPNC are reduced to two methods: limiting the duration of plasma maintenance (100-600ns) and introducing negative feedback between current and voltage. The distributed feedback

is based on the use of the reactance of high voltage pulse generator (HVPG, for example, Fitch generator), which is self-consistent with the plasma resistance of the nanosecond streamer corona in a plasma chemical reactor at the time of the current maximum. Pulse compression of power in HVPG is limited by the presence of a commercially available standard base and, above all, storage and switching elements.

The energy efficiency of installations [2] created in Russia in the last decade under the leadership of Doctor PhD Alexander Ponizovsky which are capable of generating high-frequency corona discharge plasma, is not less than 75%, i.e. only 25% of energy is lost from the socket in the pulse generator, the rest is introduced into the LTNP. The equipment can change the performance and operate from a single button in automatic mode without the participation of an operator. Moreover, such installations are the only known example in the world of gas cleaning equipment with plasma chemical reactors with smoothly adjustable technical characteristics.

It is customary to express the efficiency of a plasma chemical reactor by introducing a gamma factor (G-factor), which determines the number of accumulated active particles formed during an energy deposit in a discharge of 100eV. In pulsed discharge time-dependent G-factor for the variety of particle j is given by the expression:

$$G_j(t) = N_j(t) / \int (U \cdot I)(t) dt,$$

where  $N_j$  is the total number of particles varieties j (integral for the volume of discharge), accumulated by the moment of time t; U- and I – time-dependent voltage and discharge current.

For coaxial type reactors, the average  $G_j(t) = 2-3$ .

The task of a plasma chemical reactor, for example, during gas purification, consists precisely in the activation of impurity molecules, which in this case necessarily enter into further chemical reactions and transformations with molecules and atoms of oxygen and nitrogen in the air, i.e. are converted.

The theoretical limit of the specific energy density introduced into the gas without significant heating and, accordingly, breakdown (level 0.03 eV/molek. or 130J/dm<sup>3</sup>), is determined based on the assumption of the possibility of simultaneous activation (excitation, dissociation and/or ionization) of all oxygen and nitrogen molecules contained in a unit volume of air.

All physico-chemical processes occurring in the plasma of a nanosecond gas discharge can be divided into three time intervals:

1.  $\Delta t \approx 10^{-15}$ s – at this time interval, the processes of excitation of atoms and molecules by electron and photon shock are completed;
2.  $\Delta t \approx 10^{-13}$ s – at this time interval, the processes of ionization and dissociation of atoms and molecules are completed;
3. Up to  $\Delta t \approx 10^{-3}$ s, depending on the composition of the gas, temperature and pressure – the stage of active chemical processes and reactions.

It follows from claim 3 that in order to maintain the continuity of chemical processes and plasma chemical reactions in a 1 meter long reactor at a flow rate of 1m/s, the required pulse frequency is at least 1000 Hz, and from claim 2 that for standing air, the shape of the active particle concentration growth curve should correspond to the shape of the voltage pulse front.

For reactions between valence-saturated molecules (the atoms included in the molecules have a completely filled outer electron shell), the activation energy is close to the dissociation energy and is 100-200 kJ/mol (1.04-2.08eV/molecule). Reactions of atoms (or radicals) with molecules proceed with intermediate values of activation energy (0.42÷1.04eV /molecule). Reactions between atoms and radicals (or between radicals) occur with activation energy close to zero.

In pulsed corona discharge plasma in E/N fields at  $150 < T_d < 300$  the electron energy distribution corresponds, with reservations, to the Druvistein distribution with a maximum possible value of about 20eV, while the average electron energy is less than 8eV. The electron energy required for dissociation, excitation and ionization of nitrogen and oxygen molecules and atoms, as well as water vapor, is in the range from 1.1 to 20eV. The paper [3] concludes that it is possible to control the selectivity of plasma chemical processes by changing the electron energy distribution function. At the same time, some reactions acquire a super equilibrium character. In turn, the distribution function itself changes under the influence of various factors. Thus, the distribution function depends on the chemical composition of the working gas, the degree of ionization, the magnitude and spatial distribution of electric and magnetic fields, their dependence on time, the distribution of molecules by internal degrees of freedom, the geometry of the discharge etc.

It should be noted that acts of ionization are always accompanied by acts of excitation. At electron energies greater than 10-15eV, mainly electronic levels are excited.

The main elementary processes in low-temperature air plasma are presented in table 1.

Table 1. The main elementary processes in low-temperature air plasma

№	Process type	Diagram of a typical process
1	ionization	$e + N_2(X^1\Sigma_g^+) \rightarrow 2e + N_2^+$
2		$e + N_2(A^3\Sigma_u^+) \rightarrow 2e + N_2^+$
3		$2N_2(A^3\Sigma_u^+) \rightarrow N_4^+ + e$
4		$O + h\nu \rightarrow O^+ + e$

5	recombination	$e + N_2^+ \rightarrow N + N$
6		$e + N_4^+ \rightarrow N_2 + N_2$
7		$N_2^+ + O_2^- \rightarrow N_2 + O_2$
8		$e + O^+ + N_2 \rightarrow O + N_2$
9		$e + O^+ \rightarrow O + h\omega$
10	adhesion	$e + O_2 + N_2(O_2) \rightarrow O_2^- + N_2(O_2)$
11		$e + O_2 \rightarrow O^- + O$
12		$e + O \rightarrow O^- + h\omega$
13	excitation	$e + N_2(X^1\Sigma_g^+) \rightarrow e + N_2(A^3\Sigma_u^+)$
14		$e + N_2(X^1\Sigma_g^+) \rightarrow e + N_2(C^3\Pi_u)$
15		$e + N_2(\vartheta = 0) \rightarrow e + N_2(\vartheta \neq 0)$
16	recharge	$N_2 + O_2^+ \rightarrow N_2^+ + O_2$
17		$N_2^+ + N_2 \rightarrow N_2 + N_2^+$

At a peak power injected into a gas volume of, for example, 15 nm<sup>3</sup> per pulse duration of 100 ns at the level of 10 MW and a pollution concentration of 10 ppm, the energy density turns out to be equal to 100 eV/ molecule of pollution, which is an order of magnitude higher than the volume of gas required for activation and effective conversion. Most of the energy is spent on elastic collisions (the vibrational and rotational energy of the particles increases), in which it is dissipated, since in the future such particles transfer their energy to heating gas molecules.

In the flow gas at a concentration of impurities, for example, 0.1% (1000 ppm) for an energy density of 100eV per 1 molecule of pollution, thousand fold air exchanges is possible for 1 hour of operation, i.e. it is permissible to pass 15 nm<sup>3</sup>/hour through a plasma chemical chamber with a volume of 15 nm<sup>3</sup>.

A two-stage approach was used to model the conversion process in PPC [4]. At the first stage, the production of active particles occurs as a result of the interaction of the streamer with gas molecules. On the second, radicals, ions, excited molecules and atoms react, including with impurities.

Consider for HPPNCD only the preliminary and first stages.

At the preliminary stage, before the pulse is applied in the interval, there is a current of a stationary positive corona generated by a high-voltage voltage source [5]. With interelectrode distances of more than 25 mm from one tip, the average current value is 50 μA, which for a long multi-pointed linear electrode with a step between the tips of 5 mm gives an average linear current value of about 7mA/m [6]. Under the condition of using a coaxial tip electrode, which was in long-term operation, the current according to our direct measurements for n\*1000 points (where n = 1-6) was 0.25 mA/m. Thus, the embedded charge is 0.25 \* 10<sup>-3</sup>KL/s from one meter of the length of the corona electrode.

Such a charge during the time between 1ms pulses corresponds to the number of electrons 1.5 \* 10<sup>12</sup> or a density of 1.5 \* 10<sup>11</sup>e/nm<sup>3</sup> \* s, and with a characteristic time of 1ns, positively and negatively charged ions arise in the interval (mainly due to the adhesion of electrons in accordance with the data of Table 2).

N <sub>0</sub>	Element	Sticking Energy	Note
1	O	1,46 (2,2)	Reference data At T=0 C [7]
2	O <sub>2</sub>	0,44	
3	O <sub>3</sub>	2,0	
4	N	-0,6	
5	NO	0,9	
6	NO <sub>2</sub>	2,43 (4,0)	
7	NO <sub>3</sub>	3,7 (3,9)	
8	H <sub>2</sub> O	0,9	
9	OH	1,83	
10	CO <sub>2</sub>	3,8	

Fig. 1. Table. Electron sticking energy

In [8], it is experimentally shown that avalanche points do not form in a resonant homogeneous field with a positive charge, and the decrease of charged particles due to ion-ion recombination is determined by the expression:

$$n(t) = n_0 / (1 + n_0 b t), \text{ where } b = 10^{-13} \text{ m}^3/\text{c}.$$

It follows from this that at atmospheric pressure, the loss of charge carriers during the time between 1ms pulses will be no more than 1.5%. Of course, this does not mean that there were so many electrons in total, in fact hundreds of thousands of times more, because their lifetime without interactions with the environment under normal

conditions is close to 1ns, but the average number of charged "fighters" crossing the interelectrode gap corresponds to the above value.

### 3. Experimental results

At the first stage, the total number of electrons introduced into the gas per pulse can be estimated based on the current waveforms in various reactor chambers. For example, Figure 1 shows an oscillogram of current and voltage pulses in a reactor chamber with a volume of 12 dm<sup>3</sup> with a long corona electrode of 1000 mm, and Figure 2 shows a photo of a streamer discharge.

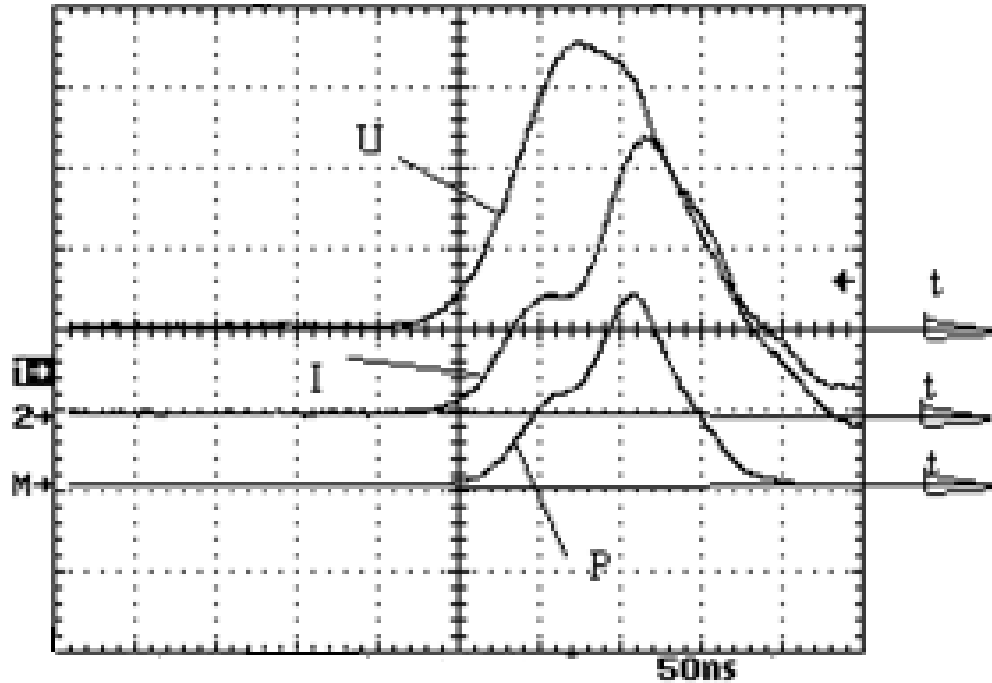


Fig. 2. Waveforms of pulses generated in a cylindrical reactor chamber

Waveforms of pulses generated in a cylindrical reactor chamber

U -20kV/div, I - 50 A/div, power introduced into gas P - 3 MW/div, T - 50ns/div

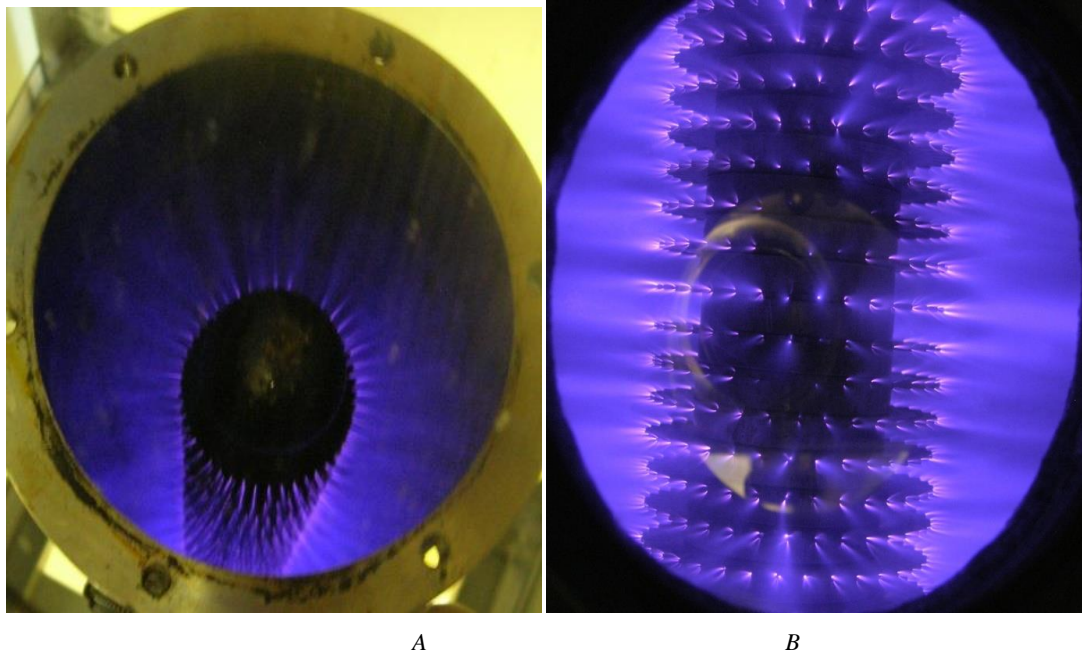


Fig. 3. Photos of a streamer discharge in a reactor chamber with a volume of 12 dm<sup>3</sup>A-view from the bottom end, B-view perpendicular to the axis of the HV electrode

An oscillogram of current and voltage in a flat electrode system is shown in Fig. 4.

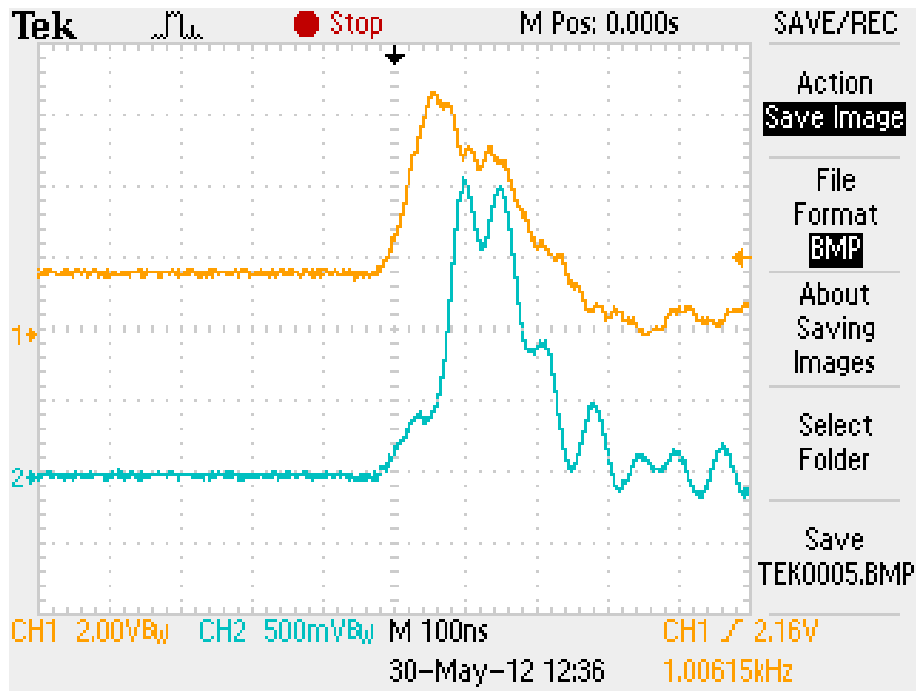


Fig. 4. Waveforms of pulses generated in a 3 D reactor chamber Scales: U - 25kV/div, I - 50 A/div, T - 100ns/div

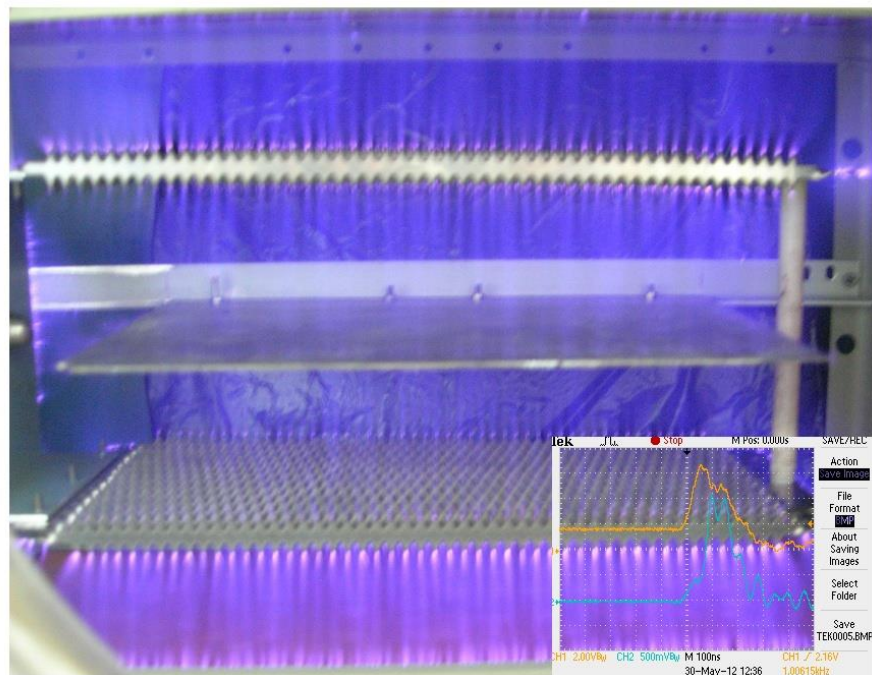


Fig. 5. Photo of a streamer discharge in a 3D reactor chamber

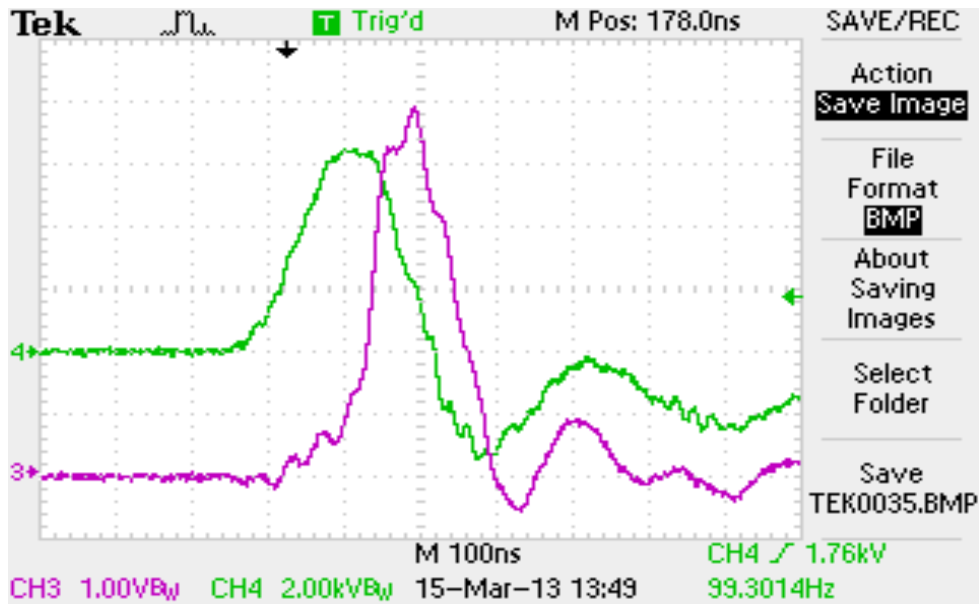


Fig. 6. Waveforms of current and voltage pulses generated in a cylindrical 4-tube reactor chamber with a length of 1500mm  
 $U = 25.5 \text{ kV/div}$ ,  $I = 100\text{A/div}$ ,  $T = 100 \text{ ns/div}$ ,  $f = 200 \text{ Hz}$ ,  $I_{\text{max}} = 630\text{A}$ ,  $P_{\text{max}} = 35 \text{ MW}$ ,  $O_3 = 46,2 \text{ eV/mol}$

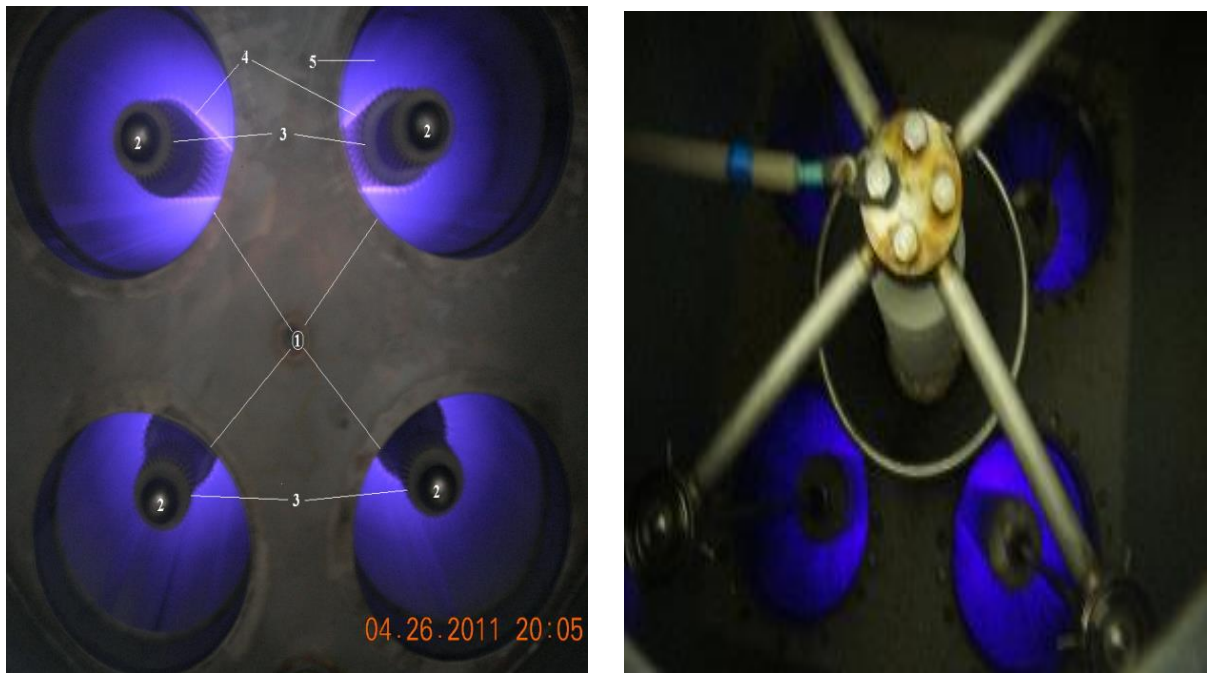


Fig. 7. Photos of a streamer discharge in a reactor chamber with a plasma volume  $100 \text{ dm}^3$ . A - bottom view, B - top view

More than 90% of the energy stored in the capacitors goes into gas,

The current integrals of Fig.3 and Fig.5 are in the range of  $(1,2-6,0) \cdot 10^{-5} \text{ Kl}$ , i.e. current carriers are of the order of  $(0,8-4) \cdot 10^{14}$  secondary electrons generated by an electric field during radiation exchange in the gas volume is  $7-12 \text{ dm}^3$ . If we take  $10^{-8} \text{ Kl}$  as the charge of a single streamer [9], then during the pulse, the gas gap is bridged by almost every streamer, but with different current values (from 10 to 100 or more  $\mu\text{A}$ ).

The transport cross-section of electron scattering in the streamer head (g) on primarily neutral nitrogen and oxygen molecules is at the level of  $(3-30) \cdot 10^{-16} \text{ cm}^2$  for electrons with the average energy is about 8eV. Moreover, the scattering cross-section for oxygen is several times larger than for nitrogen. Since there is at least 3.5 times more nitrogen in the air, we assume as a first approximation that the electron scattering cross-sections for nitrogen and oxygen are the same and depend only on the electron energy. Then the total probability of collisions of electrons with air molecules is  $P = 2g/k$ , where k is a coefficient depending on the pressure and temperature of the air.

$P = 2(3-30) \cdot 10^{-16} / k$ . We assume roughly  $k = 0.3 \cdot 10^{-16}$  [McDaniel], then  $P = 20-200 \text{ cm}^{-1}$ , which corresponds to the experimentally measured length of plasma oscillations equal to 0.05mm [10].

The energy of primary electrons is pumped, first of all, into the vibrational and rotational levels of gas molecules. Moreover, the temperature of the particles increases sharply at the moment when the streamer bridges the gap, Fig. 8 [11].

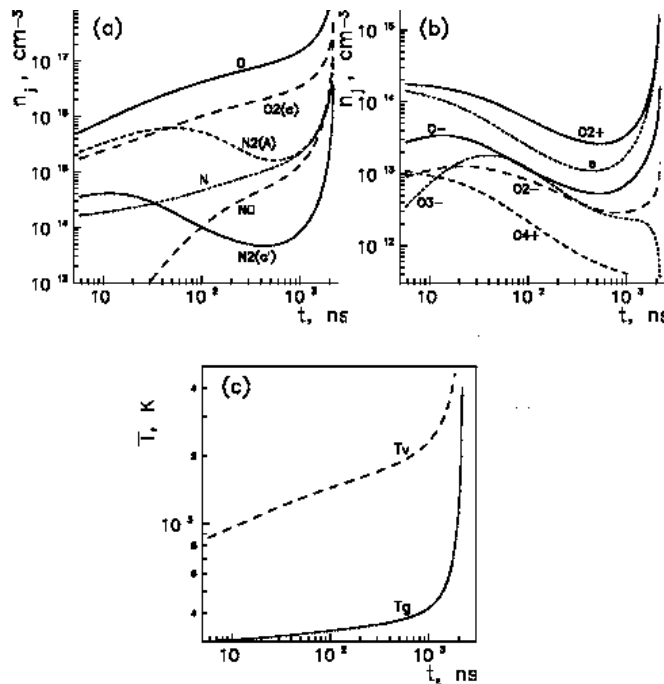


Fig. 8. The concentrations of neutral (a) and charged (b) plasma components and vibrational and translational temperatures (c) for the applied voltage  $UD$  19 kV

In [12], the average temperature of gases in the streamer channel of a positive DC streamer corona was estimated from the rotational spectrum (0.0) of the band of the second positive molecular nitrogen system at about 450 K.

#### 4. Energy density of a nanosecond streamer discharge

It is known from the literature that the maximum energy density introduced into an independent volumetric discharge without a spark breakdown lasting up to 1 ms is at the level of  $0.3 \text{ J/cm}^3 = 1.08 \text{ W} \cdot \text{h} / \text{nm}^3 = 0.07 \text{ eV/molecule}$ . (At 1ns to  $0.8 \text{ J/cm}^3$ ). The concentration of charged particles in a conventional streamer discharge in the streamer head is  $10^{16}$ - $10^{17}/\text{nm}^3$  (Fig. 9), and in a nanosecond streamer discharge it can reach a value of  $3 \cdot 10^{17}/\text{nm}^3$  [13], i.e. it is equated to the best parameters of a gas-discharge excimer laser. The probability of scattering the energy of the primary electron on the pollutant particle in one pulse at the concentration of the latter at the level of 10000ppm is less than 1%, therefore, the main interaction of the pollutant particles already occurs with ions, radicals and active molecules and atoms of oxygen and nitrogen ( $\text{N}_2\text{A}_3$ ,  $\text{N}_2\text{a1}$ ,  $\text{O}_2.\text{a1}$ , ions  $\text{O}^-$ ,  $\text{O}_2^-$ ,  $\text{O}_3^-$ ,  $\text{O}_2^+$ ,  $\text{O}_4^+$ ). Relative concentrations of positive ions of other sorts ( $\text{N}_2^+$ ,  $\text{N}_4^+$ ,  $\text{N}_2\text{O}_2^+$ ) are small, because these ions quickly turn into others [14]. At work [15] it is shown that the pulsed corona discharge can be divided into three phases related to the production of radicals and excited species: (i) primary streamer, (ii) earlier part of secondary streamer and (iii) later part of secondary streamer. It is shown that phase (iii) is inefficient for the production of most of the radicals and excited species. Moreover, the "secondary" streamer with a "cut tail" is most responsible for the production of active particles. Therefore, a short pulse is desirable for efficient production of radicals and excited species to cut off the ineffective later part of the secondary streamer, which corresponds to the second maximum current on the oscillogram when the streamer touches the grounded electrode. OH-radicals reach their maximum concentration near the end of the current pulse.



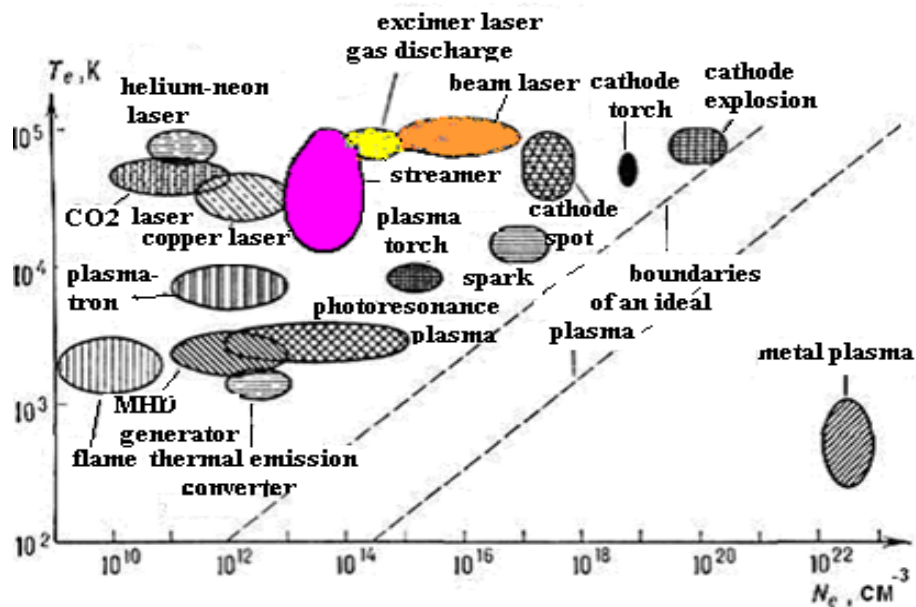


Fig. 9. Parameters of low-temperature plasma

The average specific power density of energy release in the PPNC gas discharge space exceeds the level of 100 W/dm<sup>2</sup> versus 4 - 10 W/dm<sup>2</sup> for glow discharge plasma (PGD) and DBD, respectively, and its smooth regulation in accordance with the irradiation object, it is provided by changing the frequency and, if necessary, the output voltage of the high-voltage source. Record energy deposits were achieved in [16] in the volumetric discharge stage with a short voltage pulse front and nanosecond pulse duration, reaching 800 MW/cm<sup>3</sup> (homogeneous field) in a pulse against 0.2-0.3 MW/cm<sup>3</sup> for 50-100ns PPNC pulses (inhomogeneous field) and 0.01 MW/cm<sup>3</sup> for a flare type of microwave discharge generated by a standard magnetron.

The theoretical limit of introducing energy into the gas by the electric field of the streamer head with a voltage  $E = 350$  kV/cm is the value  $eE^2/2 = 8.85 \cdot 10^{-12} \cdot 10^{14} \cdot \nu^2 / \text{m}^2 \cdot \text{f/m} = 5420 \text{ J/m}^3 = 5.42 \text{ J/dm}^3$ , which is about 50 times less than that of energy-intensive pulse capacitors and  $5 \cdot 10^4$  times less than in the channel of the lightning leader stage with a concentration of charged particles  $10^{20}/\text{ндм}^3$ .

## 5. Conclusions

Thus, it follows from the above that promising technologies using low-temperature HPPNCD plasma have not only a number of advantages over other sources of low-temperature atmospheric pressure plasma, such as high electron flux density, pulsed power and record energy transfer coefficient of the source into the plasma, but also contain a number of technical and physical limitations on the generation and introduction of energy into a gaseous medium for the purpose of initiating and controlling plasma chemical reactions.

### Acronyms/Abbreviations:

LTNP - low-temperature non- equilibrium plasma  
 DBD - dielectric barrier discharge  
 PPC - pulse-periodic corona  
 HPPNCD - high power pulse-periodic nanosecond corona discharge  
 PGD - glow discharge plasma  
 HVPG - high voltage pulse generator

### The main units and ratios used are:

$E$  - energy, W\*h;  $1 \text{ J} = 0.624 \cdot 10^{19} \text{ eV}$ ;  $1 \text{ W} \cdot \text{h} = 3600 \text{ J} = 2.2469 \cdot 10^{22} \text{ eV}$   
 $W = E/Q$  - energy density, W\*h/ nm<sup>3</sup>,  
 $1 \text{ kJ/mol} = 0.0104 \text{ eV/molecule}$ ,  $1 \text{ W} \cdot \text{h/ nm}^3 = 0.8359 \text{ eV/molecule}$   
 $1 \text{ eV/mol} = 1.2 \text{ kWh/m}^3 = 0.00432 \text{ J/m}^3 = 4.3 \text{ J/cm}^3$   
 $Q$  is the volume of gas, nm<sup>3</sup>, 1 nm<sup>3</sup> of air contains  $2,688 \cdot 10^{22}$  molecules  
 $P$  - power,  $F$  - gas flow, nm<sup>3</sup>/hour

### References / Список литературы

1. Valuev A.A., Koklyugin A.S., Norman G.E. etc. Radiation-plasma chemical methods of flue gas purification // THT, 1990. Vol. 28. № 5. P. 995.
2. Ponizovsky A.Z., Goncharov V.A., Gosteyev S.G. Optimization of parameters of electrophysical installations for air purification, // Electrical Engineering, 1993. Vol. 64. № 3. Pp. 52-58.



3. *Vlasov V.V.* Physical-chemical processes in low-temperature plasma (fundamentals of plasma chemistry) // Kharkiv, 2011.
4. *Bityurin V.A., Mokhov, G.V., Filimonova E.A.* The Conversion of naphthalene in the gas initiated by a pulsed corona discharge // XXXIV International (Zvenigorod) Conference on Plasma Physics and CTF, February 12 – 16, 2007.
5. *Ponizovskiy A.Z., Gosteyev S.G.* Probe Measurements of Parameters of Streamers of Nanosecond Frequency Crown Discharge // ISSN 1063-7788, Physics of Atomic Nuclei, 2017. Vol. 80. № 11. Pp. 1–7.
6. *Kozlov B.A., Solov'ev V.I.* Current Limit multi-apex corona // Technical physics, 2006. Vol. 76, V. 7. Pp. 1-7.
7. *Vedeneev V.I., Gurvich L.V., Kondratiev V.N. etc.* The energy of breaking chemical bonds. Ionization potentials and electron affinity // Handbook. M., from the USSR Academy of Sciences, 1962. P. 215.
8. *Stishkov Y.K., Samusenko, A.V., Subbotsky A.S. etc.* Experimental studies of pulsed corona discharge in air // ZhTF, 2010. Vol. 80, V. 11. P. 21-28.
9. *Bazelyan E.M., Raizer Yu.P.* Spark discharge // M., MIPT Publishing House, 1997. 320 p.
10. *Messi G., Barkhop E.* Electronic and ion collisions // M., I.L., 1958. 604 p.
11. *Naidis G.V.* Simulation of streamer-to-spark transition in short non-uniform air gaps // J. Phys. D: Appl. Phys. 32 (1999) 2649–2654. Printed in the UK.
12. *Shcherbakov Yu.V.* IX Symposium "Electrical Engineering 2030" // report 7.05. May, 2007. Pp. 29-31.
13. *Bazelyan E.M. and Raizer Yu. P.* Spark Discharge // Boca Raton, FL: CRC Press. 1997.
14. *Tardiveau P. et al.* Diffuse mode and diffuse-to-filamentary transition in a high pressure nanosecond scale corona discharge under high voltage // 2009 J. Phys. D: Appl. Phys. **42** 175202 (11pp) doi: 10.1088/0022-3727/42/17/175202.
15. *Ryo Ono et al.* Effect of pulse width on the production of radicals and excited species in a pulsed positive corona discharge // Journal of Physics D: Appl. Phys. V. 44. N. 48, 2011.
16. *Alekseev S.B., Gubanov V.P., Tarasenko V.F. etc.* Volumetric pulse discharge in an inhomogeneous electric field at high pressure and a short voltage pulse front // Quantum Electronics. 34. № 11, 2004.